Modeling and multi-objective optimization of low-frequency vibration-assisted chemical machining using central composite design in response surface methodology

J.Rahmani[a] , M.M.Mohammadi[b*] , R.Khamedi[c]

[a]*Jaber Rahmani. Mechanical engineering faculty, department of engineering, university of Zanjan, Zanjan, Iran;* [b]*Mohammad Mostafa Mohammadi. Corresponding author. Mechanical engineering faculty, department of engineering, university of Zanjan, Zanjan, Iran;* [c]*Ramin Khamedi. Mechanical engineering faculty, department of engineering, university of Zanjan, Zanjan, Iran; and Department of Mechanical Engineering, School of Engineering and Applied Science, Khazar University, Baku, Azerbaijan*

Mohammad Mostafa Mohammadi. Corresponding author. Mechanical engineering faculty, department of engineering, university of Zanjan, Zanjan, Iran E-mail: dr.mohammadi@znu.ac.ir, Mobile number:

Modeling and multi-objective optimization of low-frequency vibration-assisted chemical machining using central composite design in response surface methodology

Abstract. Increasing the etching rate is one of the main optimization targets in the chemical machining (CM). Traditionally, this target is fulfilled by some costly techniques like selecting stronger etchants and increasing the etchant concentration. Also, other methods like increasing the etchant temperature and stirring the etchants by agitators are employed for increasing the etching rate. One of the advantages of these methods is reduction of the consumption of acidic etchants which results in the cost reduction and making an eco-friendley process. In this article, a systematic experimental study is performed on vibration-assisted CM of copper. In this technique, the workpiece vibrates in the etchant during the CM. For evaluating the performance of machining, effects of amplitude and frequency of vibrations, along with the temperature and concentration of acidic etchant, on material removal rate, surface roughness and machining undercut are studied experimentally. The experiments are designed by Central Composite Design (CCD) in Response Surface Methodology (RSM). Also, multi-objective optimization is performed by defining a desirability function. The optimal vibro-assisted process parameters are temperature 60 □C, etchant concentration 600 g/l, vibration frequency 25 Hz, and vibration amplitude 1.5 mm, to get optimal outputs on the desired parameters.

Keywords: chemical machining; surface roughness; material removal rate; undercut of machining; copper; response surface methodology.

1 Introduction

Chemical machining (CM) is a nontraditional manufacturing process in which the machining is performed by chemical solvation of workpiece material in an etchant [1, 2]. Surface machining of copper is one of the most important applications of the CM process and is used for the fabrication of printed circuit boards (PCBs), mesoscale heat exchangers, and decorative devices, etc. [3]. Material removal rate (MRR), Surface finish and geometric accuracy of the workpiece are important output parameters of CM.

A low MRR is a challenge in the CM. To overcome this problem, researchers focused on the modification of etchants, their composition and the other effective parameters. Some researchers made parametric studies on CM of various metals in different etchants. They utilized DOE approaches like Taguchi and RSM for empirical analysis of the process and optimization of its input variables. They investigated the influence of process parameters like etchant concentration and temperature, and machining time on MRR, surface roughness, edge deviation and dimensional accuracy. Most of these researches commented that the MRR and surface roughness increased with increase of machining time, etchant concentration and etchant temperature[4-7]. However, the exact behaviour depends on workpiece material, etchant composition and machining condition and some researchers demonstrated different affects for the input variables[8-10]. The machining inaccuracy and edge deviation usually decreases with decrease of machining temperature and increase of machining time. However the dependence of machining accuracy and edge deviation to the etchant concentration is not straight forward [8, 11].

Some researchers focused on the effect of etchant composition on CM. For example Patil et al. [12], investigated the effect of etchant substance, and its concentration and temperature, on MRR and dimensional accuracy in CM of Monel 400 alloy. They commented that the accuracy and MRR depend on the type of etchant and workpiece geometry. Çakır [13] used ferric chloride as the etchant substance for the chemical machining of St37 rods. The steel rod was rotating in the etchant during machining. He investigated the effect of concentration and temperature of etchant, and workpiece rotational speed on the machining surface roughness and material removal rate. He observed that higher etchant concentration increases the etching rate but reduces the dimensional accuracy. Ruhela et al. [14] investigated the effect of different

etchant compositions, along the etchant temperature and machining time on the etching depth and surface roughness of stainless steel workpiece.

Some investigators have modified the chemical machining set-up to increase the performance of machining. For example, Gandhi and Chanmanwar [15] utilized an air aspirator machine for generating the air bubbles in the etching tank and creating turbulence in the etchant solution. They studied the effect of workpiece position in the etching tank on the MRR of chemical machining for copper and stainless steel sheets. They remarked that the uniformity of the etching depends on the positioning of the workpiece in the etchant tank. Saraf and Sadaiah, [16] designed a photochemical machining process for the fabrication of a novel cardiovascular stent on Steel 316. They applied ultrasonic vibrations to the etchant and increased the MRR by 2.7 times. Youn and Yang [17] employed ultrasonic agitation for the chemical machining of copper fine cylindrical rods. They concluded that ultrasonic agitation of the etchant can enhance the material removal rate along with the surface smoothness of the workpiece. Bahrami et al. [18] investigated the level of residual stresses and the fatigue strength of the workpiece in chemical machining. In this investigation, the aluminum workpiece was rotated during the etching. They demonstrated that rotational chemical machining leads to higher surface smoothness and fatigue strength and lower residual stresses on the workpiece respect to the traditional turning process. Jian Wang et al. [19] investigated the laser scribing as an important process for trimming away the maskant material in chemical machining. They suggested that laser scribing is an efficient method which can quickly and effectively remove the maskant and results in shortening the manufacturing time and enhancement of the manufacturing quality in chemical milling

The above-mentioned methods for enhancing the MRR like increasing the etchant concentration, selecting stronger etchants or stirring the etchant, encounter some

difficulties in mass production like increasing the corrosion rate of the etching tank and the cost of the etchant substance. In this article, vibration-assisted CM is performed on copper. In this process, the workpiece is vibrated in the etchant during the machining process. The vibration direction is perpendicular to the workpiece surface. It is predictable that employment of the vibration may increase the MRR however the magnitude of this enhancement is not identified. The other question which is addressed here is how the low frequency vibration affects the surface roughness and undercut of the workpiece. A novel experimental study based on the RSM method is performed for evaluating the effect of amplitude and frequency of vibration along with etchant concentration and temperature on MRR, surface roughness and undercut in machining. Central composite design (CCD) is utilized for designing empirical experiments. Finally, the multi-objective optimization is performed for selecting the input parameters in a way that the MRR is maximized, while the surface roughness and machining undercut are minimized.

2 Materials, Equipment and procedure

Chemical machining is the controlled chemical dissolution of the workpiece material by contact with a strong reagent, called etchant. In vibro-assisted chemical machining, the workpiece is vibrated in the etchant during chemical machining. Experimental setup was shown in Fig. 1. Single directional mechanical vibration is applied to the copper workpiece via an eccentric vibrator (Fig. 2. a). The vibrator converts the rotational movement of the AC electric motor to linear movement of the shaft. The workpiece is attached to the shaft and submerged in the etchant. The frequency of vibration equals the rotational speed of the electric motor which is adjusted by a frequency inverter. The vibration axis is parallel with the normal axis of the machining surface. The vibration amplitude depends on the adjusted eccentric distances

of connecting part in Fig. 2. The identified holes in the connecting part have a distinct distance from the central axis of the connecting shaft and determines the amplitude of vibration.

“Fig. 1.”

“Fig. 2.”

The etchant tank consists of two cylindrical enclosures which were made of 316 stainless steel (Fig. 2. b). The chemical machining was carried out inside the internal cylinder which was surrounded by electrically heated water at various temperatures (40-60 □ C). The thermostat has ±1 □ C accuracy and received its control signal from a temperature sensor which is placed in the etchant.

2.1 Materials and procedures

The workpiece material was high-purity copper and the material’s chemical composition has been given in Table 1. The thickness of the substrate was1mm and was cut to the size of 30 mm × 30 mm.

“Table 1. “

The machining region was a 10 mm length square and prepared by covering other regions of the workpiece with a polymer masking material. Before masking, the cleaning and dewaxing processes were performed by acetone. After washing and drying, the polymer masking was applied to the workpiece. Fig 3 represents the workpiece before and after applying the maskant.

"Fig. 3."

The chemical machining was performed in ferric chloride solution as one of the most relevant etchants for copper [15]. $FeCl_3$ solution was obtained by dissolving the $FeCl_3(H_2O)_6$ powder in deionized water. The temperature was controlled with 1 °C resolution. The machining time was 15 minutes and was kept constant for all the experimental runs.

3 Experimental design and optimization methodology

As mentioned in the introduction, the object of the experimental study was to determine the effect of etchant temperature and concentration, along with workpiece vibration frequency and amplitude on process output parameters including MRR, surface roughness, and the amount of undercut. The selected output parameters determined the performance of the chemical machining. The design of experiments was done by the central composite design (CCD) method based on response surface methodology (RSM). RSM includes a collection of statistical and mathematical procedures utilized in defining of a mathematical relationship between some input variables denoted by $x_1, x_2, x_3,..., x_K$ and response of interest, y. Generally, such a mathematical relationship is approximated by a low-degree polynomial function [20]. For example, the general second-order polynomial function may be represented by equation 1.

$$y = c_0 + \sum_{i=1}^{n} c_i x_i + \sum_{i=1}^{n} c_{ii} x_i^2 + \sum_{i,j=1; j\langle i}^{n} c_{ij} x_i x_j \qquad (1)$$

Here, y is the response parameter. The terms c_i and c_{ij}, are the first- and second-order regression coefficients. RSM method enables one to evaluate the effect of each input variables and their interactions on the output parameters. Also, the empirical

mathematical model is obtained relating input variable to output parameters using RSM. This model is used for the optimization of the machining conditions.

3.1 Design of experiments by CCD

Adequate experiments are necessary for fitting Eq. 1 and for extracting the unknown regression coefficients. Usually, a second-order model is enough for representing the relation between the input variables of the experiments and the output response. second-order models can be fitted by some experimental designs which are called second-order designs. The most popular of all second-order designs is the central composite design (CCD) which consists of a two-level factorial design with centre points, and is completed with a set of axial (or star) points to assess the curvature of the second-order model. Maximum efficiency is achieved when the axial points are placed a specific outside of the original factor range. The distance of centre of the design space with each factorial point is ±1 coded unit while the distance of the centre of the design space from an axial point is ±α. The value of α depends on the type of offered CCD and on the number of independent variables [20]. In the present study, the value of α was 1. The design expert software was utilized for designing the experiments and analysing the obtained results. The actual values of the input variables are selected based on the previous researches [12, 21, 22] and shown in Table 2.

"Table 2."

Thirty-seven experiments were included in the following sections: (I) Sixteen runs by the two-level factorial design, (II) one centre point and its five repeats to determine the curvature and pure errors (caused by replicating experiments) and (III) Sixteen runs for eight axial points. The designed experiments are summarized in table 3.

"Table 3."

The sources of process parameters with P-values less than 0.05 are considered to have a significant contribution to the measured values.

3.2 Analysis of variance (ANOVA)

For evaluating the model adequacy, an analysis of variance is performed. By this analysis some statistical quantities like sequential p-value, lack of fit p-value, deterministic coefficient R^2, adjusted R^2, and precision adequacy are calculated for evaluating the model's precision and adequacy. For an acceptable model, the sequential p-value should be smaller than 0.05, and the lack of fit p-value should be more than 0.05. Also, the difference between deterministic coefficient R^2 and adjusted R^2 should be smaller than 0.2, also, the quantity of precision adequacy should be more than 4 [23].

3.3 Optimization methodology

After extracting the functional relationships between the input variables and outputs, the multi-objective optimization was performed by combining the responses into a single objective function, called the desirability function. The desirability function, $D(y)$, usually is a (weighted) mean of n specific desirability functions, $d_i(y_i)$, one for each response parameter, y_i. Each $d_i(y_i)$ value is converted from associated response y_i and scaled to be between 0 and 1. The value of zero for the desirability function indicates an unacceptable response level and 1 points out that the optimal level of associated response is achieved. The general form of desirability function may be represented by equation 2:

$$D(y) = \left(d_1(y_1)^{k_1} \times d_2(y_2)^{k_2} \times \ldots \times d_n(y_n)^{k_n}\right)^{\frac{1}{\sum_i k_i}} \qquad (2)$$

where y_i denotes the determined value of response *i*, $d_i(y_i)$ is the converted desirability value of i'th response and k_i represent the relative importance of response *i* compared to others [24]. In our problem, we assumed that all responses have the same importance, thus *D(y)* becomes a geometric mean of all "*n*" transformed responses without weights. In consequence, to optimize the responses simultaneously, we were looking for the values of input variables (x_i) that maximize *D(y).* This was performed in design expert software which makes the numerical optimization of desirability function by hill-climbing technique [23].

4 Results and discussion

For better understanding and interpreting the empirical results, the chemical reactions during the machining of copper in $FeCl_3$ etchant solution are reviewed. The chemical machining of copper in $FeCl_3$ has been investigated by [25] previously. Accordingly, during the machining of copper, three chemical reactions take place. The first reaction is $Cu + Fe^{(3+)} + 3Cl^- \rightarrow CuCl_3^{(2-)} + Fe^{(2+)}$ which takes place on the workpiece surface. This reaction is continued with the second reaction i.e $CuCl_3^{2-} + Fe^{3+} \rightarrow Cu^{2+} + Fe^{2+} + 3Cl^-$.

The second reaction causes the insertion of to the etching solution and formation of $CuCl_2$ in the solution. The third reaction is related to the formation of *CuCl* passive layer on the workpiece surface and is represented by the equation $Cu + Fe^{3+} + 3Cl^- \rightarrow CuCl + Fe^{2+} + 2Cl^-$. The formation of *CuCl* passive film leads to the decrease of material removal rates with machining times [25]. When the original copper surface contacts the etchant, the machining rate is maximum. This is due to the fact that there is no *CuCl* film on the surface of copper at the start of the machining. By progressing the chemical machining and formation of the passive *CuCl* film, a diffusion

barrier forms on the copper surface, and to continue the machining, the Fe^{3+} should diffuse through the film, which decreases the machining rate.

4.1 Material removal rate (MRR)

For measuring MRR, the weight difference of the workpiece before and after the machining was measured and divided by the machining time. The weight difference was measured by a precise digital mass scale with a resolution of 0.001g. The experimental results were fed to RSM and the empirical model relating the MRR to the process parameters was extracted as equation 3:

$$\begin{aligned} MRR\times 10^3 = {} & 6.6525 + 0.69165\times B + 2.5325\times C + 3.19925\times D + \\ & 3.16356\times AC + 1.26019\times AD + 1.21019\times BC + 2.20644\times CD + \\ & 1.26896\times C^2 + 3.33571\times D^2 + 1.02269\times ACD + 0.961062\times BCD + \\ & 3.38231\times A^2C - 1.25531\times A^2D + 3.38356\times AB^2 \end{aligned} \quad (3)$$

where *A, B, C,* and *D*, are the etchant temperature, etchant concentration, vibration frequency and vibration amplitude, respectively. Eq. 3 reveals that MRR depends mainly on the etchant temperature, workpiece vibration amplitude and frequency. Also, it depends on the interactions of these variables. For evaluating the efficiency of the model, analysis of variance (ANOVA) was performed, the results were shown in table 4. The ANOVA analysis includes the evaluation of some statistical parameters like P-value, F-value, sum of squares, and adjusted and predicted R^2.

Upon the ANOVA and the reported P and F-values, the parameters *B, C, D, AC, AD, BC, BD, CD, C², D², ACD, BCD, A²C, A²D, AB²* have significant effect on the MRR. Also, the predicted R^2 has a reasonable agreement with adjusted R^2, because their difference is less than 0.2 [20]. Based on the empirical model (Eq. 3) the response surfaces for MRR were plotted and demonstrated in Fig. 4. As shown in Fig. 4 the material removal rate rises by increasing the temperature, but this change is small.

Temperature rise leads to an almost linear increment of MRR. In fact, rate of material removal depends on the rate of chemical reactions in the etchant and the resultant solvation of the workpiece. By the increase of temperature, the chemical activity of the etchant increases, which results in faster diffusion of Fe^{3+} ions in the passive layer *CuCl* [25].

"Table 4. "

"Fig. 4 **"**

Fig. 4(a) shows that by increases of concentration, initially, MRR increases and then decreases. Fig. 4(b) represents the effects of vibration amplitude and frequency on MRR. As indicated by Fig. 4(b), MRR always increases with the increase of vibration frequency. However, with increasing the amplitude, initially, MRR decreases and then increases. The enhancement of MRR by mechanical vibrations may be related to the increase of the contact energy between Fe^{3+} ions and the passive CuCl layer which causes the higher diffusion rates of the Fe^{3+} ions into the CuCl layer.

4.2 Surface Roughness

Machining surface roughness was obtained by Insize standard roughness scale IS 4131. The experimental results were fed to the RSM and the empirical model relating the roughness values to the process parameters is extracted as equation 4:

$$Ra = 1.58889 + 0.28375 \times A - 0.11675 \times B - 0.82015 \times C - 0.05945 \times D \quad (4)$$

ANOVA analysis was performed for the evaluation of model adequacy. Table 5 shows the analysis of variance for surface roughness. All the parameters are effective however vibration frequency is the most effective parameter for surface roughness [20].

“Table 5.”

Surface responses for roughness were plotted in Fig 5(a) and (b). Fig 5(a) and (b) illustrate that an increase in the etchant temperature leads to the increase of surface roughness, however an increase in the etchant concentration, vibration frequency and amplitude results in the reduction of the surface roughness. In fact, increasing the temperature results in non-uniform material removal rate which is the main cause of increase of surface roughness [13]. On the other hand, movement of the workpiece in the etchant usually leads to decrease of surface roughness due to enhancement of uniformness in material removal rate [8]. The vibration frequency and the etchant temperature are more effective on the surface roughness than the other parameters.

“Fig. 5 “

4.3 Undercut in machining

The undercut is one of the drawbacks of chemical machining, where the actual dimensions of machining regions are more than the desired dimensions. Thus, to achieve dimensional accuracy, undercut must be minimized by selecting the optimum process parameters. The undercut is shown in Fig. 6 [4].

“Fig. 6 “

The undercut was calculated by equation (5).

$$undercut = \frac{b-a}{2} \qquad (5)$$

Where *a* and *b* are the dimensions measured before and after the machining. The experimental results for undercut were introduced to RSM. The undercut mathematical model was obtained as equation 6:

$$undercut = 0.0869757 + 0.044715 \times A - 0.005955 \times B + 0.018245 \times C + 0.017395 \times D \quad (6)$$

Table 6 shows the analysis of variance for the undercut. According to the ANOVA, the significant parameters of the machining undercut is concentration. Vibration frequency and vibration amplitude and etchant temperature, have a weak effect on the undercut [20].

"Table 6."

The response surfaces for undercut were plotted by Design Expert software and represented in Fig. 7. As indicated in Fig. 7(a) temperature had more strong amplitude on undercut effect on the undercut than concentration.

"Fig. 7"

The results reveal that the temperature is the most effective parameter on undercut of machining. With the increase of temperature, the undercut always increased. The undercut is occurred when the etchant solution etches the workpiece both vertically and laterally once it has permeated through a feature or aperture in the photoresist. Increase of temperature results in enhancement of kinetic energy of ferric chloride molecules. By increase of kinetic energy of etchant molecules, the number of effective molecular collisions between the etchant and the workpiece is increased both laterally and vertically, which results in increase of undercut [26].

By the increase of concentration the undercut initially increased and then decreased. The effect of temperature and concentration were similar to the results obtained by Saraf et al. [27]. The effect of vibration amplitude and frequency were shown in Fig. 7(b). As seen in this figure, by the increase of vibration frequency and amplitude the undercut initially decreased and then increased. However, the variation of the undercut due to the vibration frequency and amplitude was very small. It is worth mentioning that application of mechanical vibrations along the normal axis of the machined surface resulted in enhancement of material removal rate along with a small change of undercut of machining. Indeed, the vibrational motion of the workpiece in direction of its normal axis, increases the number of strong and effective collisions between the reactant molecules in vertical direction, however it does not change the collision state in lateral direction effectively. This results in increase of MRR with a small change of undercut defect.

4.4 multi-objective optimization

Maximizing the MRR along with minimizing the surface roughness and machining undercut was the purpose of multi-objective optimization, which was performed in design expert software using the desirability approach. In defining the desirability function, as in the other similar researches, we assumed that all the three responses have the same importance [28].

Fig. 8 shows optimization plots for output variables. From the graph, it is clear that in the optimum condition the values of MRR, surface roughness and undercut are 0.028, 0.87, and 0.16 respectively. These outputs were achieved when the etchant temperature, etchant concentration, and vibration frequency and amplitude were, 600 g/l, 25 Hz, and 1.5 mm respectively. The results are represented in table 7. For validation of the optimization results, three experimental runs were performed in the

optimum condition and the average output variables were measured. The results are represented in table 7.

“Fig. 8”

“Table 7. “

5 Conclusion

In this article, the chemical machining process was performed on a copper workpiece. The workpiece was vibrated in ferric chloride as the etchant solution during the machining. For investigating the effects of vibrations on the machining performance, an experimental study was defined. In this study, etchant temperature and concentration, along with vibration frequency and amplitude were selected as the input variables. The process outputs were MRR, surface roughness, and undercut in machining. The experiments were designed by central composite design, and the empirical models were obtained by the RSM method. Analysis of variance (ANOVA) was performed for evaluating the empirical models and the following conclusions are remarked:

1- Analysis of variance of the extracted empirical models shows that the selected input variables can successfully simulate and predict the variations of MRR, surface roughness and undercut in vibro-assisted chemical machining of copper.

2- Employing the mechanical vibrations to the copper workpiece during chemical machining, can result in the increase of MRR and machining undercut along with a decrease in surface roughness. The parameter of frequency was more effective on the machining performance than the parameter of vibration amplitude.

3- Maximizing the machining performance parameters including MRR, surface roughness and machining undercut is an optimization aim. In this research, the optimal setting for achieving the maximum MRR, and a minimum amount for surface roughness and undercut was determined with 74.5 % of desirability. In the optimum condition, the etchant temperature, etchant concentration, and vibration frequency and amplitude were found to be, 60° C, 600g/l, 25 Hz, and 1.5 mm respectively.

Based on the results, the application of low-frequency vibrations in the chemical machining of copper resulted in an improvement in overall performance of machining and this founding may be examined for other metals.

Nomenclature

y	Output response
c_i	First order regression coefficients
c_{ij}	Second order regression coefficients
x_i	Input parameters
a	Mask hole diameter
b	Machined hole diameter
A	Temperature
B	Concentration
C	Frequency
D	Amplitude

References

[1] Jain, V.K. "Advanced machining processes", Allied publishers., (2009).

[2] Rohith, R., Ruthvik, G. and Raju, K., et al. "Chemical machining process-a review", *Proceedings on Engineering*, **4**(1), pp. 33-36 (2022).

[3] Raut, M. A., Kale, S. S. and Pangavkar, P. V. "Fabrication of micro channel heat sink by using photo chemical machining", *Int J New Technol Res,* **5**(4) , pp. 72-75 (2019).
[4] Wagh, D., Dolas, D., and Dhagate, M. "Experimental investigation of photochemical machining on Inconel 600 using ferric chloride", *International Journal of Engineering Research & Technology,* **4**(2) , pp. 289-293 (2014).
[5] Wangikar, S. S., Patowari, P. K., and Misra, R. D. "Parametric optimization for photochemical machining of copper using overall evaluation criteria", *Materials Today: Proceedings,* **5**(2), pp. 4736-4742 (2018).
[6] Kamble, B., Utpat, A. and Misal, N., et al. "Effect of Process Parameters on Response Measures of Cartridge Brass Material in Photo Chemical Machining", in *Techno-Societal 2020*: Springer, pp. 995-1003 (2021).
[7] Gangmei, G., Kumar, J. and Debnath, T., et al. "Parametric Analysis for Machining of Stainless Steel AISI (SS-430) Using Photo Chemical Machining", in *Recent Advances in Mechanical Engineering*: Springer, pp. 829-837 (2021).
[8] Mazarbhuiya, R. M. and Rahang, M. "Parametric Study of Photochemical Machining of Aluminium Using Taguchi Approach", in *Advances in Mechanical Engineering*: Springer, pp. 497-504 (2020).
[9] Ibrahim, A., Abdulwahhab, A. and Shabeeb, A. "Influence of fecl3 on material removal rate and surface roughness in chemical machining process", *Kufa Journal of Engineering,* **10**(1), pp. 44-55 (2019).
[10] Gandhi, S. V. and Rahul, M. C. "Experimental investigation of wet chemical machining and optimization of process parameters using grey relational analysis for SS 316L", *Materials Today: Proceedings,* **5**(1), pp. 23908-23916 (2018).
[11] Mazarbhuiya, R. M. and Rahang, M. "Parametric Optimization in Photochemical Machining of Aluminium Using Taguchi Method", in *IOP Conference Series: Materials Science and Engineering*, **491**(1): IOP Publishing, p. 012033 (2019).
[12] Patil, D. H., Thorat, S. B and Khake. R.A., et al."Comparative study of FeCl3 and CuCl2 on geometrical features using photochemical machining of monel 400", *Procedia CIRP*, **68**, pp. 144-149, (2018).
[13] Çakır, O. "Chemical Machining of St37 Rod Using Etchant Substance FeCl3", *Acta Physica Polonica A*, **135**(4), pp. 583-585 (2019).
[14] Ruhela, V., Ansari, M.I., Jadhav, P.V., et al. "An experimental investigation of photo chemical machining process for stainless-steel material by using different etchants", *Materials Today: Proceedings,* (2023).
[15] Gandhi, S. V. and Chanmanwar, R. "A Study of Variation in MRR Influenced by Work Piece Positioning on Copper and Stainless Steel During Wet Chemical Machining", in *International Conference on Advances in Thermal Systems, Materials and Design Engineering (ATSMDE2017)*, (2017).
[16] Saraf , A. R. and Sadaiah, M. "Photochemical machining of a novel cardiovascular stent", *Materials and Manufacturing Processes,* **32**(15), pp. 1740-1746 (2017).
[17] Yang, M. Y. and Youn, J. W. "Ultrasonic-assisted chemical machining of fine rods", *Wear,* **145**(2), pp. 303-313 (1991).
[18] Bahrami, P. Khoshanjam, A. and Azizi, A. "Evaluation of Fatigue Behavior and Surface Characteristics of Novel Machining Process: Rotary Chemical Machining (RCM)", *ADMT Journal,* **14**(3), pp. 17-24 (2021).

[19] Wang, J., Sun, Q. and Sun, P. "Research Status and Prospect of Laser Scribing Process and Equipment for Chemical Milling Parts in Aviation and Aerospace", *Micromachines*, **13**(2), p. 323 (2022).
[20] Khuri, A. I. and Mukhopadhyay, S. "Response surface methodology", *Wiley Interdisciplinary Reviews: Computational Statistics*, **2**(2), pp. 128-149 (2010).
[21] Mumbare, P. and Gujar, A. "Multi objective optimization of photochemical machining for ASME 316 steel using grey relational analysis", *International Journal of Innovative Research in Science, Engineering and Technology*, **5**(7), pp. 12418-12425 (2016).
[22] Chanmanwar, R., Balasubramaniam, R., Sapkal, S.U., et al. "Fabrication of Microchannels on SS-304 and Copper by Wet Chemical Etching and Comparison of Topographies", in *International Conference on Advances in Thermal Systems, Materials and Design Engineering*, (2017).
[23] Whitcomb, P. J. and Anderson, M. J. "optimizing processes using response surface methods for design of experiments", *RSM simplified*, CRC press, (2004).
[24] Akçay, H. and Anagün, A. S. "Multi response optimization application on a manufacturing factory", *Mathematical and Computational Applications*,**18**(3), pp. 531-538 (2013).
[25] Jian, C., Jusheng, M. and Gangqiang, W., et al. "Effects on etching rates of copper in ferric chloride solutions", in *2nd 1998 IEMT/IMC Symposium (IEEE Cat. No. 98EX225)*, IEEE, pp. 144-148 (1998).
[26] Yadav, S., Saraf, A. and Sadaiah, M. "Analysis of Undercut for SS304 in Photochemical Machining", in *International Conference on Communication and Signal Processing 2016 (ICCASP 2016)*, Atlantis Press, pp. 284-289 (2016).
[27] Saraf, A. R., Sadaiah, M. and Devkare, S. "Optimization of photochemical machining", *International Journal of Engineering Science and Technology*, **1**(3), pp. 7108-7116 (2011).
[28] Nemati, B., M. M. Mohamamdi, and R. Moharrami. "Multi-objective optimization of electrochemical finishing for attaining the required surface finish and geometric accuracy in the hole making process", *Scientia Iranica* (2023).

Captions of Figs:

Fig. 1. Vibro-assisted chemical machining setup, a. Schematic illustration of the equipment, b. The constructed setup.

Fig. 2. a: Mechanical vibrator, b: Schematic chemical machining reactor

Fig. 3. the workpiece before (a) and after masking (b).

Fig. 4. a. Effect of temperature and concentration on MRR, b. Effect of vibration frequency and amplitude on MRR

Fig. 5. a. effect of temperature and concentration on surface roughness, b. Effect of vibration frequency and amplitude on surface roughness

Fig. 6. Schematic view of machining undercut

Fig. 7. a. effect of temperature and concentration on undercut, b. Effect of vibration frequency and amplitude on undercut in machining

Fig. 8. optimization plots for output variables

Captions of Table:

Table 1. composition of workpiece material

Table 2. Actual values of input variables

Table 3. experimental layout plane designed by CCD

Table 4. Results of ANOVA for material removal rate

Table 5. Report of ANOVA for surface roughness

Table 6. Report of ANOVA for undercut

Table 7. Report of ANOVA for undercut

Figures:

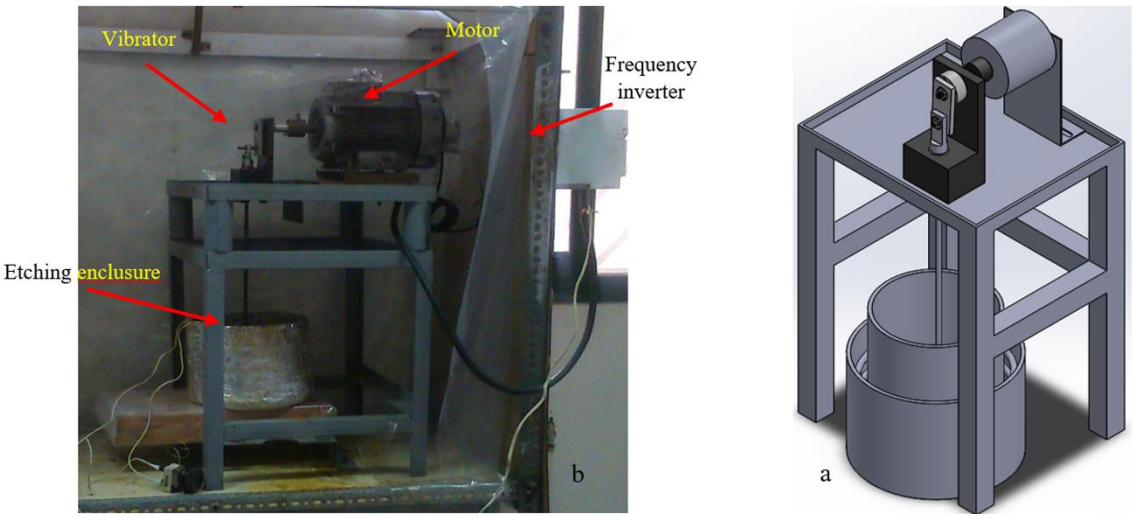

Fig. 1.

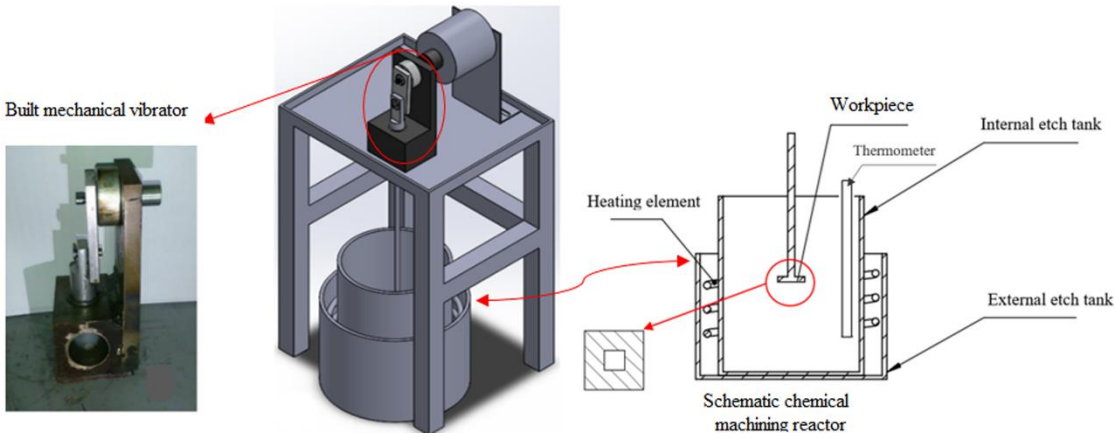

Fig. 2.

Fig. 3.

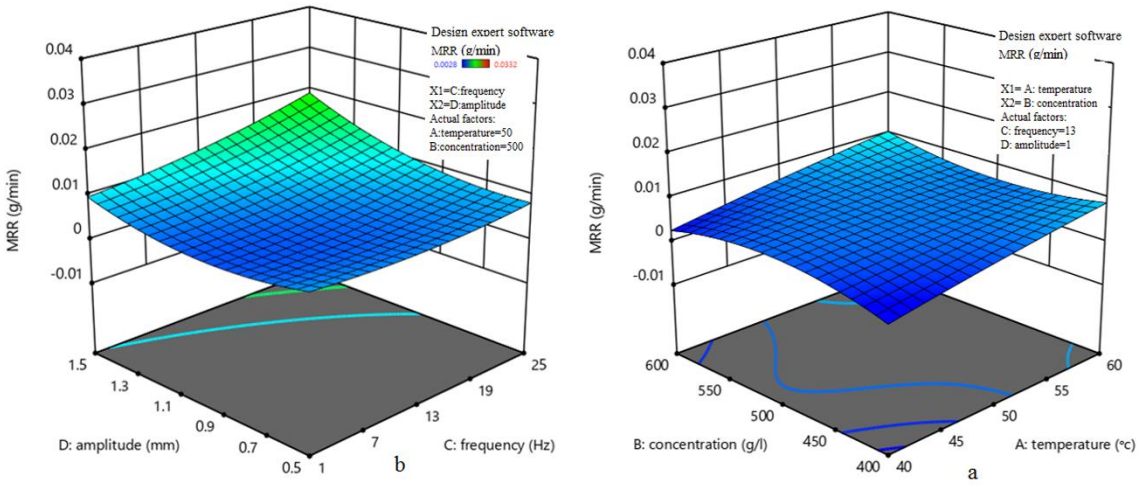

Fig. 4.

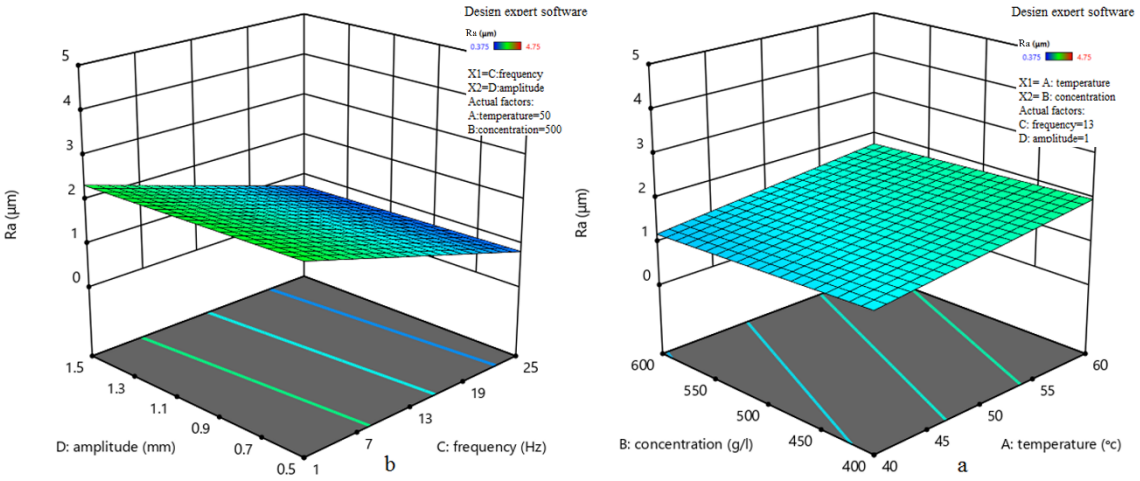

Fig. 5.

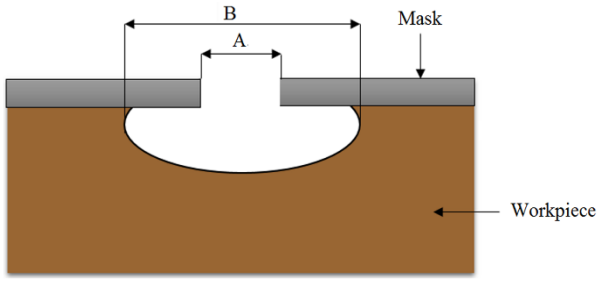

Fig. 6.

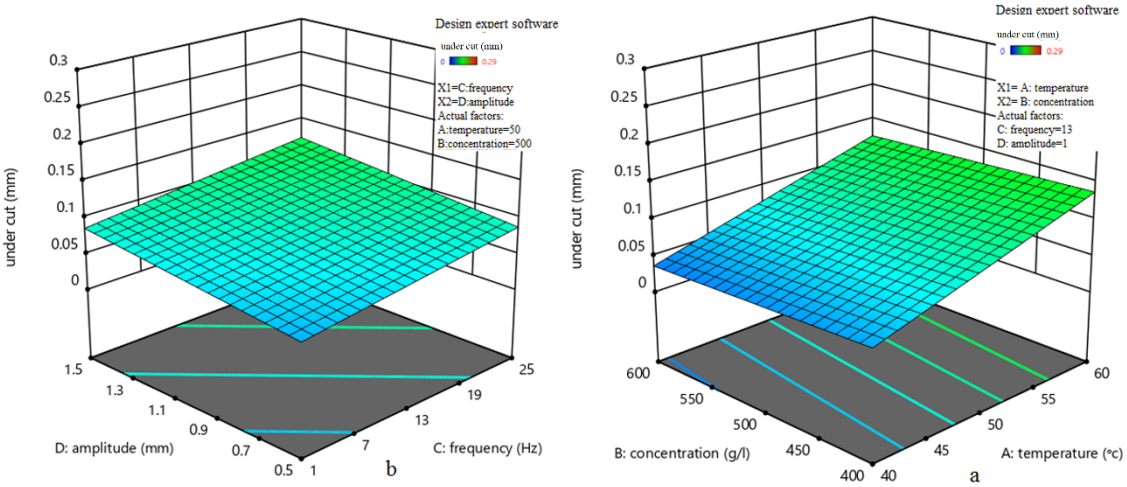

Fig. 7.

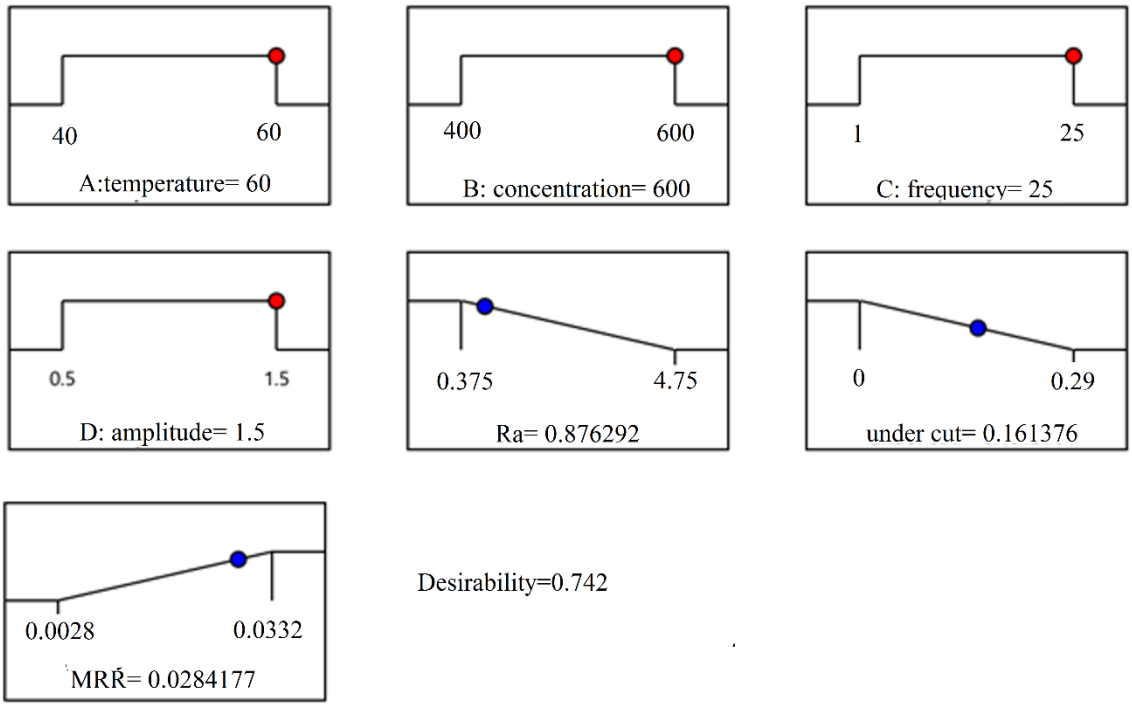

Fig. 8.

Table:

Table 1.

Components	cu	pb	si	Others
Value (%)	99.9	0.034	0.027	< 0.05

Table2.

Number	Factors	Level 1	Level 2	Level 3
1	*A* = Temperature (□c)	40	50	60
2	*B* = Concentration (g/l)	400	500	600
3	*C* = Frequency (Hz)	1	13	25
4	*D* = Amplitude (mm)	0.5	1	1.5

Table 3.

std	run	*A*=Temperature (□ c)	*B*=Concentration (g/L)	*C*=Frequency (Hz)	*D*=Amplitude (mm)
16	1	60	600	25	1/5
10	2	60	400	1	1/5
14	3	60	400	25	1/5
19	4	60	500	13	1

27	5	50	500	25	1
15	6	40	600	25	1/5
34	7	50	500	13	1
23	8	50	600	13	1
5	9	40	400	25	0/5
11	10	40	600	1	1/5
25	11	50	500	1	1
31	12	50	500	13	1/5
6	13	60	400	25	0/5
8	14	60	600	25	0/5
2	15	60	400	1	0/5
22	16	50	400	13	1
36	17	50	500	13	1
1	18	40	400	1	0/5
35	19	50	500	13	1
12	20	60	600	1	1/5
33	21	50	500	13	1
9	22	40	400	1	1/5
29	23	50	500	13	0/5
21	24	50	400	13	1
18	25	40	500	13	1
3	26	40	600	1	0/5
20	27	60	500	13	1
17	28	40	500	13	1
24	29	50	600	13	1
26	30	50	500	1	1
32	31	50	500	13	1/5
4	32	60	600	1	0/5
28	33	50	500	25	1
30	34	50	500	13	0/5
13	35	40	400	25	1/5
37	36	50	500	13	1
7	37	40	600	25	0/5

Table 4.

Source	Sum of Squares	df	Mean Square	F-value	p-value	
Model	0.0014	19	0.0001	74.01	<0.0001	significant
A-temperature	1.071E-06	1	1.071E-06	1.08	0.3133	
B-concentration	9.568E-06	1	9.568E-06	9.65	0.0064	
C-frequency	0.0000	1	0.0000	25.86	<0.0001	
D-amplitude	0.0000	1	0.0000	41.28	<0.0001	

AB	5.096E-08	1	5.096E-08	0.0514	0.8234	
AC	0.0002	1	0.0002	161.44	<0.0001	
AD	0.0000	1	0.0000	25.62	<0.0001	
BC	0.0000	1	0.0000	23.62	0.0001	
BD	7.259E-06	1	7.259E-06	7.32	0.0150	
CD	0.0001	1	0.0001	78.53	<0.0001	
A^2	7.348E-07	1	7.348E-07	0.7408	0.4014	
B^2	7.938E-07	1	7.938E-07	0.8003	0.3835	
C^2	8.149E-06	1	8.149E-06	8.22	0.0107	
D^2	0.0001	1	0.0001	56.77	<0.0001	
ACD	0.0000	1	0.0000	16.87	0.0007	
BCD	0.0000	1	0.0000	14.90	0.0013	
A^2C	0.0000	1	0.0000	36.91	<0.0001	
A^2D	5.043E-06	1	5.043E-6	5.08	0.0376	
AB^2	0.0000	1	0.0000	36.94	<0.0001	
Residual	0.0000	17	9.919E-07			
Lack of Fit	8.967E-06	5	1.793E-6	2.73	0.0718	Not significant
Pure Error	7.895E-06	12	6.579E-07			
Cor Total	0.0014	36				
R^2=0.9881			Adjusted R^2=0.9747		Predicted R^2=0.8722	

Table 5.

Source	Sum of Squares	df	Mean Square	F-value	P- value	
Model	15.41	4	3.85	5.13	0.0026	significant
A-temperature	1.61	1	1.61	2.14	0.1528	
B-concentration	0.2726	1	0.2726	0.3631	0.5510	
C-frequency	13.45	1	13.45	17.92	0.0002	
D-amplitude	0.0707	1	0.0707	0.0942	0.7609	
Residual	24.02	32	0.7508			
Lack of Fit	14.02	20	0.7010	0.8408	0.6466	Not sinificant
Pure Error	10.00	12	0.8337			
Cor Total	39.43	36				
R^2=0.3907		Adjusted			Predicted	

		R^2=0.3146			R^2=0.2130	

Table 6.

Source	Sum of Squares	df	Mean Square	F-value	P- value	
Model	0.0534	4	0.0134	5.08	0.0028	significant
A-temperature	0.0400	1	0.0400	15.22	0.0005	
B-concentration	0.0007	1	0.0007	0.2700	0.6069	
C-frequency	0.0067	1	0.0067	2.53	0.1212	
D-amplitude	0.0061	1	0.0061	2.30	0.1389	
Residual	0.0841	32	0.0026			
Lack of Fit	0.0606	20	0.0030			
Pure Error	0.0235	12	0.0020	1.55	0.2193	Not sinificant
Cor Total	0.1375	36				
R^2=0.3885		Adjusted R^2=0.3121			Predicted R^2=0.1644	

Table 7.

	Ra (μm)	Under cut (mm)	MRR (g/min)
Model	0.87	0.16	0.028
Experiment	0.80	0.17	0.026

Biography:

Jaber Rahmani biography:

Jaber Rahmani has a master's degree in mechanical engineering from Zanjan University in Iran and is currently working as a Repairs and maintenance expert at seven-diamond company. Among his achievements, we can mention getting an A grade in undergraduate and graduate degrees and being selected as one of the exemplary students of the province.

Mohammad Mostafa Mohammadi is assistant professor of Manufacturing in University of Zanjan where he teaches various courses in graduate and undergraduate levels. His research interests are micro-fabrication, electrochemical manufacturing processes, and piezoelectric

transducers and energy harvesters. He obtained his B.Sc. from university of Tabriz and M.Sc. from University of Tarbiat Modares and Ph.D. from university of Tehran.

Ramin Khamedi is a professor of mechanical engineering at Khazar University, Baku-Azerbaijan. Within the last years he has been doing researches on Fractography using SEM and TEM, topology characterization using AFM and digital holography, microstructure effects on mechanical properties of steels, additive manufacturing, failure micro-mechanisms of composites, nondestructive tests including acoustic emission and digital holography, and metals forming.